MATHEMATICS FOR ENVIRONMENTAL PROBLEMS: FROM MODELLING TO APPLICATIONS

LUIS FERRAGUT AND M. ISABEL ASENSIO

1. Introduction

Fortunately, in recent decades, environmental protection has become a challenging scientific and technological task as we became aware of the need to protect the environment. The scientific and technological progress had made possible the swift industrial development, and that, in turn, has caused a myriad of environmental problems. Likewise, the scientific and technological progress must serve now to the environmental protection.

An interesting anecdote points to the insights that mathematics can offer into environmental problems: the commonly used today term *greenhouse effect* to describe human effects on the global climate, was originally coined by a mathematician, Joseph Fourier (1768-1830), in an article in 1819.

There are thousands of scientific works that examine ways in which mathematics can contribute to understanding and solving environmental problems such as pollution, global warming, biodiversity and genetic diversity (loss of species), population growth, impending losses of resources, etc. The ability to accurately understand and interpret mathematical environmental data in these critical areas through mathematical models can contribute to the health and welfare of Earth.

Most of these environmental problems operate on very different scales of space and time, and mathematical methods provide the only way such problems can be approached, with techniques of scaling, aggregation, and simplification that are essential. Numerical methods and computer technology are other two mainstays supporting mathematical models.

One of the world's most alarming processes of environmental degradation is deforestation, and one of its causes is wildfires. Natural and man-made wildfires cause a heavy environmental impact and have a significant impact on global warming by killing trees that could absorb carbon in the atmosphere. Furthermore, as forest fires devour trees and other plants, they release the carbon stored in the vegetation into the atmosphere. In turn, the effects of global warming on temperature, precipitation levels, and soil moisture have led to a worsening of wildfires around the world, with longer wildfire seasons, increasing the frequency and duration of wildfires.

In this paper we summarize some aspects of the simplified physical wildfire spread model developed by the authors and of the Geographical Information System tool specially developed to provide a real usable wildfire spread tool based on this model.

Key words and phrases. Mathematical environmental models.

Authors were supported in part by *Conserjería de Educación* of the *Junta de Castilla y León* (SA020U16) and by *University of Salamanca General Foundation*, both with the participation of FEDER.

Similarly, we outline the grounds of a wind field model developed by the authors as a key component of the wildfire spread model, but that has its own applications.

The two models we present here are just a drop in the ocean of environmental protection that the scientific progress should provide. Unfortunately, however, humans fail to listen to the scientific community warnings about the environmental destruction. In 1992, the Union of Concerned Scientists and more than 1.700 independent scientists including many Nobel laureates, signed the *World Scientists Warning to Humanity* calling to curtail environmental destruction, imploring that we cut greenhouse gas emissions and phase out fossil fuels, reduce deforestation, and reverse the trend of collapsing biodiversity. Twenty five years later, arrives the *World Scientists Warning to Humanity: A Second Notice*, with more than 15.000 signatures, evaluating the human response to that warning by exploring available time-series data. The conclusions are devastating: *"Since 1992, with the exception of stabilizing the stratospheric ozone layer, humanity has failed to make sufficient progress in generally solving these foreseen environmental challenges, and alarmingly, most of them are getting far worse"*.

2. PhyFire: a simplified physical wildfire spread model

The current version of the PhyFire model is the result of the development of a simple 2-D one-phase physical model first published in [1], based on the energy and mass conservation equations, considering convection and diffusion. In [2] radiation was incorporated to the initial model with a local radiation term, so that the model considers one of the dominant thermal transfer mechanism in wildfires, radiation. A multivalued operator representing the enthalpy was carried out in [3] to represent the influence of moisture content and heat absorption by pyrolysis. The way of taking into account radiation was modified in [4] by means of a non-local radiation term that allows the modelling of the radiation from the flame above the fuel layer, enabling to cope with the effect of wind and slope over the flame tilt.

The numerical methods used to solve the non-dimensional equations derived from the model, include finite element method combined with different finite difference schemes in time, characteristic method for the convective term, Yosida approximation for the multivalued operator and discrete ordinate method for the non local radiation equation. In addition, efforts have been made to reduce the computational cost by means of definition of active nodes and parallel computation techniques in order to become competitive compared with experimental models. This first operative model was named PhFFS (Physical Forest Fires Spread), although it appears in an international review as UoS in 2009 [5].

Since the first versions of the model, sufficient account has been taken of the issue of visualization of the simulations, in order to devise a handy tool for the final user [6]. Recently, the PhyFire model has been integrated in a Geographical Information System (GIS), specifically the commercial ArcMap 10.4 of Esri's ArcGIS Desktop suite [1], in order to attach the wildfire model to the spatial data, providing an efficient and fully operational tool over the Spanish territory [7]. This tool automates data acquisition, pre-processes spatial data, launches the model and displays

[1]ArcGIS ® and ArcMap™ are the intellectual property of Esri and are used herein under license. Copyright © Esri. All rights reserved. For more information about Esri ® software, please visit www.esri.com.

the corresponding results in the ArcMap environment. This GIS integrated simulation tool is now accessible through the url: `http://sinumcc.usal.es`. A detailed description of the development of this tool is given in Section 4.

Work has also gone into improving the feasibility of the PhyFire model with simulations of real fires in [8], and experimental fires in [9]. The simulation of experimental examples has been used to perform a global sensitivity analysis of input variables and parameters of the model allowing to conclude that the model properly reflects the most important factors affecting a wildfire spread. Besides that, the global sensitivity analysis is also the previous step to the parameter adjustment of the model. The simulation of real fires is critical in order to carry out the challenging task of the model parameter adjustment, and it is one of the main motivations of automating the simulating process by its integration into GIS in order to automate the processes of input data capture and output data visualization. On the other hand, with the objective of achieving a more helpful tool, we have also incorporated data assimilation techniques based on Kalman filter in [10], allowing to correct the approximations obtained by the model simulations and providing more realistic predictions.

The last improvement added to the PhyFire model is a flame length submodel developed to deal with the influence of wind and slope over the flame length as evidenced in [13].

Model equations. The non-dimensional equations governing the current version of the PhyFire model are,

$$\partial_t e + \beta \mathbf{v} \cdot \nabla e + \alpha u = r \quad \text{in } S \quad t \in (0, t_{max}), \tag{2.1}$$

$$e \in G(u) \quad \text{in } S \quad t \in (0, t_{max}), \tag{2.2}$$

$$\partial_t c = -g(u)c \quad \text{in } S \quad t \in (0, t_{max}). \tag{2.3}$$

The surface S where the fire occurs, is large enough so that the fire does not arrive to the boundary during the time of study $(0, t_{max})$, so we complete the problem with homogeneous Dirichlet boundary conditions and the initial conditions representing the initial fuel and temperature.

The unknowns, $e = \frac{E}{MCT_\infty}$, dimensionless enthalpy, $u = \frac{T-T_\infty}{T_\infty}$, the dimensionless temperature of the solid fuel and $c = \frac{M}{M_0}$, the mass fraction of solid fuel, are bidimensional variables defined in $S \times (0, t_{max})$, representing the corresponding physical quantities E $(J\,m^{-2})$, enthalpy, T (K), temperature of solid fuel, and M $(kg\,m^{-2})$, fuel load, respectively. T_∞ (K), is a reference temperature related with the ambient temperature measured far enough away from the fire front that $T \geq T_\infty$ in order to assure $u \geq 0$. C $(J\,K^{-1}\,kg^{-1})$, is the heat capacity of solid fuel and M_0 $(kg\,m^{-2})$ is the maximum solid fuel load, both depending on the fuel type. We shall assume that vegetation can be represented by a given fuel load M $(kg\,m^{-2})$ together with a moisture content M_v, (kg of water/kg of dry fuel). M and M_v are scalar functions defined in the surface S, where M_v depends also on the fuel type.

The multivalued operator G in Equation (2.2) represents the enthalpy which models the influence of moisture content and depends on the fuel moisture content M_v and pyrolysis temperature T_p.

The convective term, $\beta \mathbf{v} \cdot \nabla e$ in Equation (2.1), represents the energy convected by the gas pyrolyzed through the elementary control volume, where the surface wind velocity, $\mathbf{v}$, is re-scaled by a correction factor β, which can be found explained

in detail in [9]. The surface wind velocity $\mathbf{v}$ can be considered as given data or can be computed by a wind model, as for example the High Definition Windfield (HDWind) explained in the following section. The coupling of this convection model with the wind model was detailed by the authors in [3].

Although the PhyFire model is a two-dimensional model, it takes into account some important three-dimensional factors. One of these three-dimensional factors is the energy lost by natural convection in the vertical direction, represented by a zero-order term αu in the partial differential Equation (2.1) of temperature. The parameter α is related to physical quantities by $\alpha = \frac{H[t]}{MC}$, where H $(J\, s^{-1}\, m^{-2}\, K^{-1})$ is the natural convection coefficient and $[t]$ is a time scale.

Other important three-dimensional factor is the radiation from the flames above the surface where the fire takes place. The effect of the surface slope and wind is taking into account through the flame tilt in the radiation computation that depends on the flame length F, and total radiation intensity I. The radiation intensity is computed by solving the corresponding differential equation on the three-dimensional air layer over the surface S. For further details about the radiation computation see [10] and [9].

Finally, the right hand side of Equation (2.3) represents the loss of solid fuel due to combustion, that is null if the temperature is below the pyrolysis temperature, and it remains constant when the temperature of pyrolysis is reached. This constant value is inversely proportional to the solid fuel half-life time $t_{1/2}$.

Some important simplifications are assumed in the PhyFire model. The model considers only the solid phase of the combustion process: the mass fraction of solid fuel, c, is a non-dimensional variable between 0 and 1, and the maximum value of non-dimensional solid fuel temperature, u, is $u_p = \frac{T_p - T_\infty}{T_\infty}$, the non-dimensional pyrolysis temperature, where T_p (K) is the pyrolysis temperature that depends on the fuel type. The gaseous phase is parameterized through flame temperature, T_f (K), and flame length, F (m), in the radiation term r. Flame temperature depends on fuel type, but flame length also depends on wind intensity and surface slope by means of the following submodel

$$F = (F_H + F_v|v|^{1/2})(1 + (F_s s)^2)^{1/2}$$

where , F_H is a flame length independent parameter, F_v is a wind correction factor, F_s is a slope correction factor, $|v|$ is the wind strength, and s represents the slope on each point of the surface.

The three generally accepted forms of heat transfer in wildfires are conduction, convection and radiation, although the most important physical processes driving heat transfer in a wildfire are convection and radiation. In low wind conditions, the dominating mechanism is radiation [11], but when the wind is not insignificant it is convection that dominates [12]. The relative importance of radiation and convection varies from fire to fire and estimation of their exact combination is not simple, although it is possible to rule out diffusion. The PhyFire model takes into account both, radiation and convection, and allows to avoid the convective term $\beta \mathbf{v} \cdot \nabla e$ when wind conditions are negligible. The global sensitivity analysis of the PhyFire model developed in [9] allows us to conclude that the most relevant parameter in terms of rate of spread and fire thickness in low wind conditions is the mean absorption coefficient a of the radiation term, which is coherent with the importance of radiation in low wind fires. This analysis also reflects the importance

of the convection in fires driven by high winds through the relevance that the correction factor of convective term β achieves in the global sensitivity analysis of windy examples. All these assumptions provide a simplified model that only depends on several factors, that can be differentiated between model parameters and input variables. Among these can be distinguish those that depend on fuel type. The three unknown parameters are the mean absorption coefficient a, the natural convection coefficient H and the correction factor of convective term β, which must be adjusted in each case. Some of the input variables strongly affect the evolution of a fire and define different scenarios, these are the wind and the slope, the ambient temperature and fuel load, which are represented in the PhyFire respectively through the non-dimensional wind velocity $\mathbf{v}$, the height of the surface h, the fuel load M, and the reference temperature T_∞. The other input variables depend on each type of fuel: the flame temperature T_f, the pyrolysis temperature T_p, the half-life time of combustion $t_{1/2}$, the flame length parameters F_H, F_v and F_s, the heat capacity C and the fuel moisture content M_v.

Examples. Here we present some simulations of several real wildfires along different regions of the country. The wildfires simulated have diverse sizes and characteristics, both as regards topography and fuel type.

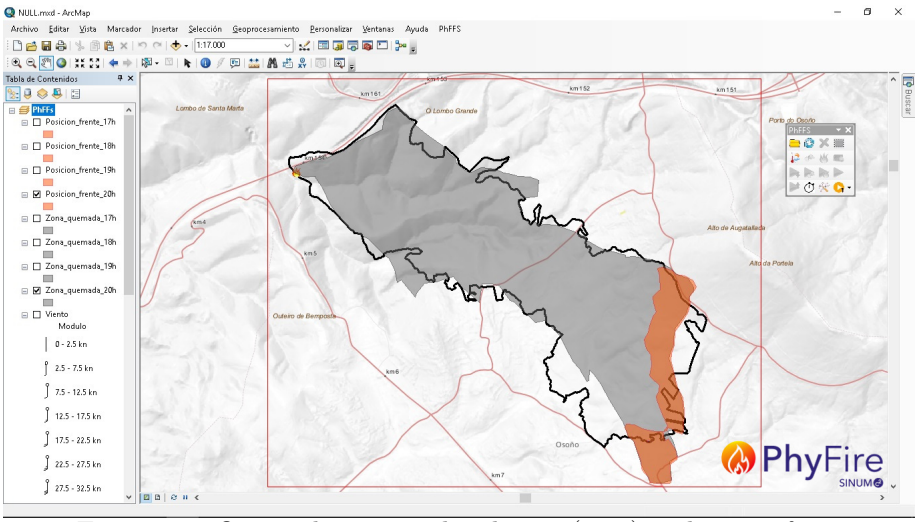

FIGURE 1. Osoño: burnt simulated area (grey) and active front (orange) after 4 hours and real perimeter (black line).

The first example corresponds to a wildfire near Osoño, Ourense province, on 17 August 2009. The fire spread and its behaviour were reconstructed and documented by the coordinator of the fire-suppression operations in [14], providing detailed information about this case. This fire destroyed 224 ha, 185 ha of forest area (83 ha were tree-covered interspersed with heath) and 39 ha of agricultural area for about 4 hours. In this case the slope is lower, the altitude ranges from 540 m (ignition point area) to 680 m (end fire area) above sea level, with a relative humidity below 25%, temperatures above 30° C, and winds about 15 km/h with gust about 25 km/h. The simulation area is a rectangle of 3.315 $m \times 2.740\,m$. In Fig. 1 we show the

simulated perimeter after 4 hours compared with the real perimeter, the similarity index obtained show substantial agreement: Sorensen similarity index $S = 0.82$, Jaccard similarity coefficient $J = 0.69$ and Kappa coefficient $K = 0.77$ [15]. The simulation results are displayed on the GIS environment developed.

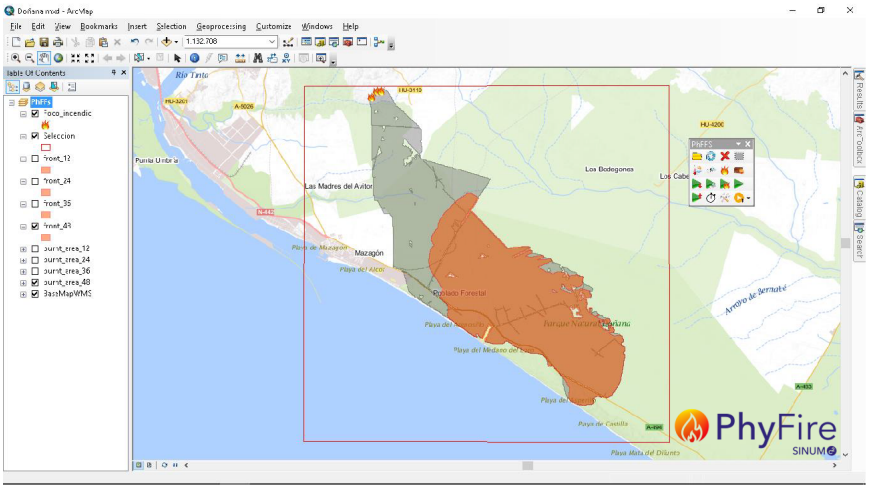

FIGURE 2. Doñana: burnt simulated area (grey) and active front (orange) after 48 hours.

The second example corresponds to a larger and more recent wildfire that hited Doñana National Park. The fire broke out in Moguer (Huelva) on 24 June 2017, burning 8486 ha (6761 ha inside the Park) during four days due to the strong winds up to 80 km/h. In this case, data were obtained from satellite images. The simulation area was a rectangle of 20300 $m \times 20000\,m$. In Fig. 2 we show the simulated perimeter after 48 hours.

3. HDWIND: A HIGH DEFINITION WIND FIELD MODEL

Wind models are a fundamental tool in the study of environmental problems such as dispersion of pollutants, fire propagation, among others. In problems where the meteorology plays an important role the resolution methods depend on the temporal and spatial scales that are chosen. With deterministic models only predictions can be made for a few days.

The HDWind is a mass consistent vertical diffusion wind field model. If the significant phenomena that we want to simulate occur in a zone, where the horizontal dimensions are much larger than the vertical one, then an asymptotic approximation of the primitive Navier-Stokes equations can be derived as in the model developed in [16, 17]. The most salient feature of this asymptotic approach is that it provides a three-dimensional velocity wind field (which satisfies the incompressibility condition in the air layer) governed by a two-dimensional equation, so that it can be coupled with the temperature surface distribution in order to take into account the thermal effects such as sea breezes. In addition, the terrain elevation information is also taken into account by the model, as well as surface roughness.

The validity of this model has the following limits: the nonlinear terms are neglected and it is assumed that the air temperature decreases linearly with the height. Besides that, the model takes into account buoyancy forces, slope effects, and mass conservation.

In the rest of the section a brief description of the wind model is included. Finally, a numerical example in a real-data scenario is presented.

HDWind model description. A complete description can be found in [16, 17]. Our model arrives from an asymptotic analysis of Navier–Stokes equations and gives a three-dimensional convective model governed by a two-dimensional equation. This model adjusts a three-dimensional velocity wind field in a layer under the influence of the topography and temperature distribution.

Consider an air velocity field $\mathbf{U} = (U, V, W)$ and a potential P satisfying the Navier–Stokes equations. We assume that the height δ is small compared to the width, and that the surface height at point $(\mathbf{x}, H(\mathbf{x}))$, is smaller than δ. We obtain the following vertical diffusion model:

$$-\partial^2_{zz}\mathbf{V} + \nabla_{\mathbf{x}} P = 0, \tag{3.1}$$

$$\partial_z P = \mu T, \tag{3.2}$$

$$\nabla_{\mathbf{x}} \cdot \mathbf{V} + \partial_z W = 0, \tag{3.3}$$

where $\mathbf{V} = (U, V)$ denotes the horizontal velocity, μ is related to buoyancy forces and T is the temperature.

Equations (3.1)-(3.2)-(3.3) together with the corresponding boundary conditions yield

$$\mathbf{V}(\mathbf{x}, z) = m(\mathbf{x}, z)\nabla_{\mathbf{x}} p(\mathbf{x}) + k(\mathbf{x}, z)\nabla_{\mathbf{x}} \hat{t}(\mathbf{x}), \tag{3.4}$$

where $m(\mathbf{x}, z)$ and $k(\mathbf{x}, z)$ are polinomial fuctions in z and $\hat{t}$ is a re-scaled temperature. The function $p(\mathbf{x})$ is a potential that satisfies the following boundary value problem:

$$\begin{aligned} -\nabla_{\mathbf{x}}(a\nabla_{\mathbf{x}} p) &= \nabla_{\mathbf{x}}(r\,\nabla_{\mathbf{x}}\hat{t}) \quad \text{in } \omega, \\ a\frac{\partial p}{\partial \mathbf{n}} &= -r\,\frac{\partial \hat{t}}{\partial \mathbf{n}} + (\delta - H)\mathbf{v}_m \cdot \mathbf{n} \quad \text{on} \quad \partial\omega, \end{aligned} \tag{3.5}$$

where $a(\mathbf{x})$ and $r(\mathbf{x})$ are functions depending on δ and $H(\mathbf{x})$. ω is a two dimensional bounded domain, representing the projection of the three dimensional geographical surface.

Summarizing, the solution $\mathbf{V}$ of problem (3.1)-(3.3) is obtained by solving the two-dimensional boundary value problem (3.5) and then $\mathbf{V}$ is explicitly computed using the expression (3.4).

In practical applications, the wind on the boundary is unknown. Instead, measurements of the wind intensity and direction are given at the points where the weather stations are placed. So we have to reformulate problem (3.5) so that the given data be the wind velocity at some fixed points.

Given E experimental measurements of the wind velocity $\mathbf{V}_i,\ i = 1, \ldots, E$, at E fixed points $P_i = (\mathbf{x}_i, z_i),\ i = 1, \ldots, E$, we look for the function $v = (\delta - H)\mathbf{v}_m \cdot \mathbf{n}$ such that the values of $\mathbf{V}(\mathbf{x}_i, z_i)$ given by the expression in (3.4) are as close as

possible to the experimental values of $\mathbf{V}_i$. The cost functional to be minimized is given by

$$J(v) = \frac{1}{2}\sum_{i=1}^{E}\int_{\omega}\rho_{\varepsilon,i}(\mathbf{x})|m(\mathbf{x},z_i)\nabla p(\mathbf{x})+k(\mathbf{x},z_i)\nabla\hat{t}(\mathbf{x})-\mathbf{V}_i|^2 d\mathbf{x}+\frac{\alpha}{2}\int_{\partial\omega}v^2 d\sigma, \tag{3.6}$$

where α is a regularization parameter and $\rho_{\varepsilon,i}$ is a suitable smoothing function.

The minimum u of the functional J is characterized by the vanishing of the first variation: $J'(u) = 0$. We refer to [18] for a general characterization of this solution using the adjoint state approach and [17] for the application to this particular case.

Example. We consider a domain located at La Serena (Chile, IV Region) (14 km $\times$ 8 km), with two weather stations: Ceaza and Cerro Grande. We use Cerro Grande measurement to estimate the wind velocity at Ceaza. Data: 25 days, 1 measurement per hour ($25 \times 24 = 600$)

FIGURE 3. La Serena (Chile, IV Region).

In Fig. 4 it is shown the results obtained by our High Definition Wind Model (in blue) versus the observed velocity at Ceaza (in red). In green is shown the observed data at Cerro Grande.

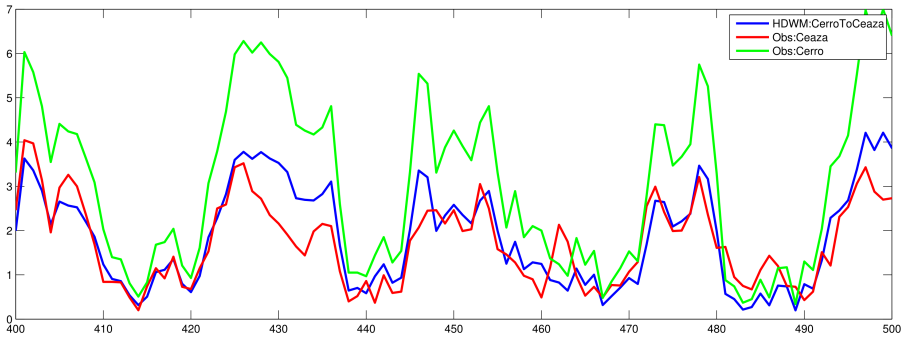

FIGURE 4. High Definition Wind Model (HDWind) vs Observed velocity at Ceaza.

4. PhyFire & HDWind: the development of a GIS tool

Both models, PhyFire and HDWind, can be compiled for any platform, and can operate either together or separately: the PhyFire model can operate with constant wind or with wind data provided by the HDWind or any other wind model. Furthermore, the HDWind model can provide wind field data from punctual meteorological data for other purposes. But in order to make these models more readily accessible to the potential end-user by providing a simple, intuitive and easy-to-use tool, both have been integrated on a GIS-based interface. This has a dual purpose, on the one hand, as we have mentioned, this provides a more accessible tool to a broader audience that might not be familiar with these models; and on the other hand, this facilitates the testing and validation process, by automating and simplifying the data acquisition process and the display of the solution. The complete simulation of either one of the physical processes integrated on the GIS interface, includes three steps: pre-processing the requested data, calculating the models and post-processing the solution. The developed tool reduces preprocessing and post-processing times and prevent input data errors.

The PhyFire and HDWind models have an interface provided through ASCII grid text files as inputs and outputs. The GIS tool chosen for the integration of our models, ArcMap 10.4 of Esri's ArcGIS Desktop suite, provides options for expanding its features through custom tools. For more information about Esri software, visit www.esri.com. The interface with both models has been developed as a Python add-in for ArcMap, that is, a customization, in this case a collection of tools on a toolbar, which plugs into an ArcGIS for Desktop application (ArcMap in this case) to provide supplemental functionality for performing customized tasks. The functionality of each tool is implemented as a script using the Python programming language and the ArcPy geoprocessing library. The PhyFire integrated in the GIS tool uses the following input data: topography, fuel load and type, weather conditions, ignition location and fire suppression tactics; and predicts the fire spread for the established time period, providing the following outputs at each time step: the burnt area perimeter and the fire front position. Likewise, the HDWind integrated in the GIS tool also uses topography, surface roughness and weather conditions, and provides a wind velocity field that is well adapted to the domain studied, defined by wind velocity. Both have been developed for its use throughout Spain, so the scope of the spatial information currently used is limited to that area. We define a common spatial reference for all the heterogeneous spatial data resources. According to Spanish regulations, the selected spatial reference is the Projected Coordinate System ETRS1989 UTM Zone 30N, except for the Canary Islands, where the Projected Coordinate System ETRS1989 UTM Zone 28N is used instead.

The first geographical resource is the base map used to identify the area in which the simulation is to be carried on, to locate the fire ignition point, as well as possible fire suppression tactics and meteorological wind data positions, and finally, to display the simulation results. The base map selected for our operating system is the Spanish Topographic Base Map provided by the © Instituto Geográfico Nacional de España (IGN) via a Web Map Service [22].

Each simulation needs three raster files corresponding to the topography, fuel type and fuel load of the study domain. For this purpose, a geodatabase has been developed containing the three maps needed for extracting the spatial information our models use.

The first map processed contains the height of the surface h required for both models. This information is provided by a Digital Elevation Model (DEM). We select the DEM also published by the IGN via a Web Coverage Service (WCS) [23] with resolution $25\,m$ and the reference system mentioned above.

The second map processed gathers all the information related to fuel type, to set the fuel type-dependent input variables for both models. Depending on the region and/or year we use the Spanish Forestry Map $1:25.000$ (MFE25) [24] combined with the Fourth Spanish National Forest Inventory (IFN4) [25] or the Spanish Forestry Map $1:50.000$ (MFE50) [26] with the information from the Third Spanish National Forest Inventory (IFN3) [27]. Both inventories have been developed by the Ministry of Agriculture, Food and Environment of the Spanish Government. The fuel type distribution managed is BEHAVE classification [28], adapted to Spanish forestry by the Nature Conservation Institute [29].

The third map processed collects all the elements involving the function of either artificial or natural fuelbreaks that affect the fire spread, only used by the PhyFire model. These data have been extracted from the Spanish Land Cover Information System (SIOSE) [30] by selecting all the surfaces where a fire cannot occur (barren land, waterbodies, transport infrastructures, etc.), providing zero load fuel data for the model.

The simulation results are displayed on the base map during the post-process step. The PhyFire model provides two types of output data: the solid fuel mass fraction c and the non-dimensional solid fuel temperature u. Comparing the output solid fuel mass fraction with the initial fuel mass fraction inputted into the model provides the state of the landscape. So for each point of the domain we can determine whether or not that specific point has been burnt. This information is transformed to a vector layer and represented on the base map in order to establish the fire perimeter at different instants, using a layer for each time step. The solid fuel temperature is also transformed into a vector layer and represented on the base map for identifying those areas burning at the indicated time step, establishing the fire front position.

FIGURE 5. Doñana: burnt simulated area (grey) and active front (orange) after 48 hours over 3D satellite image.

Similarly, the wind velocity data that the HDWind provides at different layers over the ground surface can be displayed. The resulting wind field is displayed by combining this information on a feature class, using its attributes (module and direction) for setting the corresponding colours and arrows with the right rotation.

The amount of necessary work to develop the whole system that allows to transform the mathematical models presented here into useful and accessible tool is an essential part of the model development.

Fig. 5 displayed the simulation results of Doñana fires, in the PhyFire current graphic environment, including 3D landscape images.

Acknowledgments

This work has been partially supported by *Conserjería de Educación* of the *Junta de Castilla y León* (SA020U16) and by *University of Salamanca General Foundation*, both with the participation of FEDER. Authors express their appreciation to Ignacio Juarez Relaño, chief of the Nature Protection Section of the *Junta de Castilla y León* in Salamanca and to Arsenio Morillo Rodríguez for the detailed Osoño fire data.

References

1. L. Ferragut, M. I. Asensio, R. Montenegro, A. Plaza, G. Winter, F. J. Sern, Computational Fluid Dynamics, John Wiley & Sons, Ltd., Ch. *A model for fire simulation in Landscapes*, (1996), 111–116
2. M. Asensio, L. Ferragut, *On a wildland fire model with radiation*, International Journal for Numerical Methods in Engineering **54 (1)** (2002), 137–157.
3. L. Ferragut, M. Asensio, S. Monedero, *A numerical method for solving convectionreactiondiffusion multivalued equations in fire spread modelling*, Advances in Engineering Software **38 (6)** (2007) 366–371.
4. L. Ferragut, M. Asensio, S. Monedero, *Modelling radiation and moisture content in fire spread*, Communications in Numerical Methods in Engineering **23 (9)** (2007) 819–833.
5. A. Sullivan, *Wildland surface fire spread modelling, 19902007. 1: Physical and quasi-physical models*, International Journal of Wildland Fire **18 (4)** (2009), 349–368.
6. F. Serón, D.Gutiérrez, J. Magallón, L. Ferragut, M. Asensio, *The evolution of a wildland fire front*, The Visual Computer **21 (3)** (2005), 152–169.
7. D. Prieto, M. I. Asensio, L. Ferragut, J. M. Cascón, A. Morillo, *A GIS based fire spread simulator integrating a simplified physical wildland fire model and a wind field model*, International Journal of Geographical Information Science **31 (11)** (2017), 2142–2163.
8. L. Ferragut, M. Asensio, J. Cascón, D. Prieto, Advances in Differential Equations and Applications, no. 4 in SEMA SIMAI Springer Series, Springer International Publishing, Cham, Ch. *A Simplified Wildland Fire Model Applied to a Real Case* (2014), 155–167.
9. D. Prieto, M. Asensio, L. Ferragut, J. Cascón, *Sensitivity analysis and parameter adjustment in a simplified physical wildland fire model*, Advances in Engineering Software **90** (2015), 98–106.
10. L. Ferragut, M. Asensio, J. Cascón, D. Prieto, *A wildland fire physical model well suited to data assimilation*, Pure and Applied Geophysics **172 (1)** (2015), 121–139.
11. R. Weber, *Analytical models for fire spread due to radiation*, Combustion and Flame **78 (3)** (1989), 398-408.
12. R. Weber, *Modelling fire spread through fuel beds*, Progress in Energy and Combustion Science **17 (1)** (1991), 67–82.
13. S. Arellano, J. Vega, A. Ruíz, A. Arellano, J. Alvarez, D. Vega, E. Pérez, *Foto-guía de combustibles forestales de Galicia. Versión I*, Andavira Editora, S.L., (2016).
14. A. Morillo, *Análisis del comportamiento del fuego forestal observado y simulado: estudio del caso del incendio forestal de Osoño (Vilardevós)-Verín-Ourense*. Spain: Master of advances studies work, Higher Politechnical School of Lugo, University of Santiago de Compostela. (in Spanish) (2011).

15. J. Filippi, V. Mallet, and B. Nader, *Representation and evaluation of wildfire propagation simulations*. International Journal of Wildland Fire, **23** (2014), 46–57.
16. M. Asensio, L. Ferragut, J. Simon, *A convection model for fire spread simulation*, Applied Mathematics Letters **18** (2005), 673–677.
17. L. Ferragut, M. I. Asensio, J. Simon, *High definition local adjustment model of 3d wind fields performing only 2d computations*, International Journal for Numerical Methods in Biomedical Engineering **27** (2011), 510–523.
18. J. L. Lions, *Controle Optimal de Systèmes Gouvernés par des Equations aux Dérivés Partielles*, Springer series in computational mathematics, Dunod/Gauthier-Villars, Paris, (1968).
19. J.M. Cascón, A. Engdahl Y, L. Ferragut, E. Hernández, *A reduced basis for a local definition wind model. Computer Methods in Applied Mechanics and Engineering*, Computer Methods in Applied Mechanics and Engineering **23**, (2016) 438–456.
20. W. C. Skamarock, et. al, *A Description of the Advanced Research WRF Version 3*, NCAR Technical Nore.(2008)
21. D. Barker, et.al *The Weather Research and Forecasting Model's Community Variational/Ensemble Data Assimilation System: WRFDA* American Meteorological Society. https://doi.org/10.1175/BAMS-D-11-00052.1
22. *IGN Spanish Base Map* Instituto Geográfico Nacional de España [online]. Available from: `http://www.ign.es/wms-inspire/ign-base` [Accessed May 2016].
23. *Spanish Digital Elevation Model* Instituto Geográfico Nacional de España [online]. Available from: `http://www.ign.es/wcs/mdt` [May 2016].
24. *Spanish Forestry Map* 1 : 25.000. Ministerio de Agricultura, Alimentación y Medio Ambiente [Online]. Available from: `http://www.magrama.gob.es/es/desarrollo-rural/temas/politica-forestal/inventario-cartografia/mapa-forestal-espana/mfe25.aspx` [Accessed May 2016b].
25. *Fourth Spanish National Forest Inventory* Ministerio de Agricultura, Alimentación y Medio Ambiente [Online]. Available from: `http://www.magrama.gob.es/es/desarrollo-rural/temas/politica-forestal/inventario-cartografia/inventario-forestal-nacional/` [Accessed May 2016a].
26. *Spanish Forestry Map* 1 : 50.000 Ministerio de Agricultura, Alimentación y Medio Ambiente [Online], 3 (4). Available from: `http://www.magrama.gob.es/es/biodiversidad/servicios/banco-datos-naturaleza/informacion-disponible/mfe50.aspx` [Accessed May 2016a].
27. *Third Spanish National Forest Inventory* Ministerio de Agricultura, Alimentación y Medio Ambiente [Online]. Available from: `http://www.magrama.gob.es/es/biodiversidad/servicios/banco-datos-naturaleza/informacion-disponible/ifn3.aspx` [Accessed May 2016b]
28. P. Andrews *Behave: fire behaviour prediction and fuel modellings system - burn subsystem, part 1*, Ogden, UT: U.S. Department of Agriculture, Forest Service, Intermountain Forest and Range Experiment Station, General Technical Report INT-194, (1986).
29. MAPA, *Photographic key to the identification of fuel models*, Madrid: Ministerio de Agricultura Pesca y Alimentación, Instituto para la Conservación de la Naturaleza ICONA, Technical report. [in Spanish].
30. Spanish Land Cover Information System. Instituto Geogrfico Nacional de España [online]. Available from: `http://www.ign.es/ign/layoutIn/siose.do` [Accessed May 2016].

Department of Applied Mathematics, University of Salamanca
Current address: Department of Applied Mathematics, University of Salamanca, Casas del Parque, 2, 37008 Salamanca
E-mail address: `ferragut@usal.es`

Department of Applied Mathematics, University of Salamanca
E-mail address: `mas@usal.es`